ESI

Biomimetic Polyelectrolyte-Gradient Hydrogel Electricity Generator: A Green and Portable Energy Source

Xiaofeng Pan[a], Qinhua Wang[bc], Daniele Benetti[ae]*, Lei Jin[ade], Yonghao Ni[f]*, Federico Rosei[a]*

[a] Centre for Energy, Materials and Télécommunications, Institut National de la Recherche Scientifique, 1650 Boulevard Lionel-Boulet, Varennes, Québec J3X 1P7, Canada

[b] College of Material Engineering, Fujian Agriculture and Forestry University, Fuzhou City, Fujian Province 350002, People's Republic of China

[c] Département of Chemistry, Université de Montréal, C.P. 6128, Succursale Centre-ville, Montréal, Québec H3C 3J7, Canada

[d] Institute of Fundamental and Frontier Sciences, University of Electronic Science and Technology of China, Chengdu, 610054 P. R. China

[e] Department of Chemistry, McGill University, 801 Sherbrooke Street West, Montreal, Quebec, H3A 0B8 Canada

[f] Limerick Pulp and Paper Centre, Department of Chemical Engineering, University of New Brunswick, Fredericton, New Brunswick E3B5A3, Canada

Email: daniele.benetti@inrs.ca (Daniele Benetti); yonghao@unb.ca(Yonghao Ni); federico.rosei@inrs.ca (Federico Rosei).
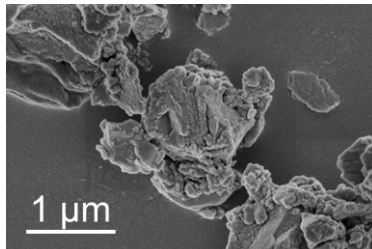
Supplementary figures

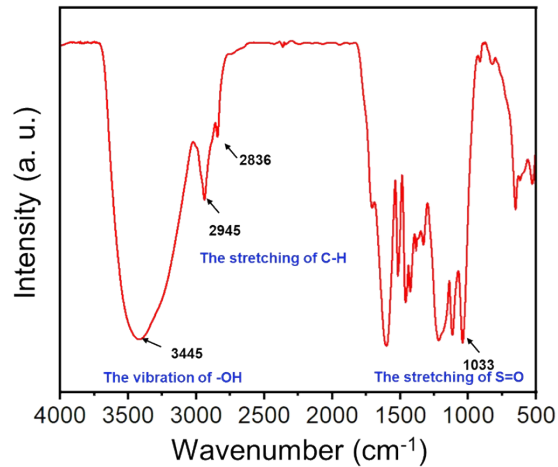**Figure S1**. The microscopic morphology of lignosulfonate sodium (LS).

Figure S2. The FTIR spectra of LS. The material used in this work present the characteristic peaks of LS, with the peak at 1033 cm−1 revealing the existence of sulfonate groups (-SO3).[1]
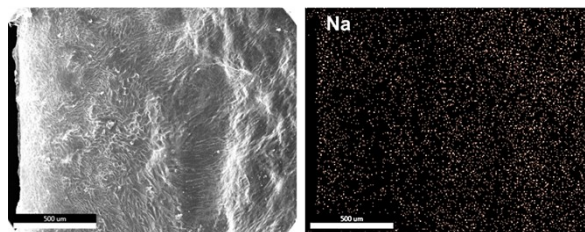

Figure S3. Microscopic morphology and Na distribution of PVA-LS hydrogel. Scale bar: 500 μm.
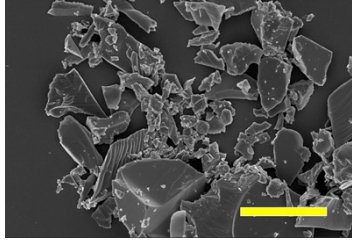
Figure S4. The microscopic morphology of quaternary chitosan (QC). Scale bar: 10 μm.
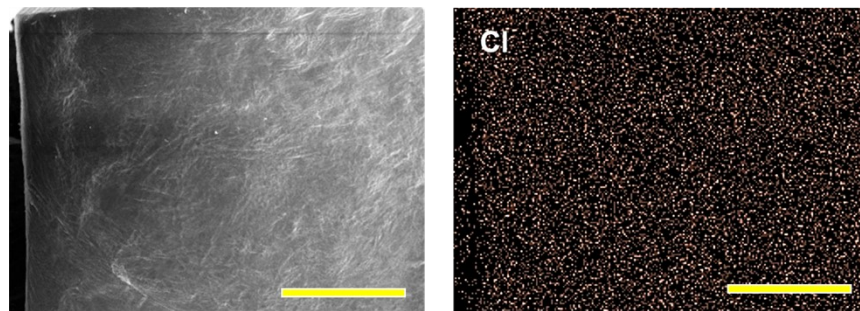

Figure S5. The microscopic morphology and Cl distribution of PVA-QC hydrogel. Scale bar: 500 μm.
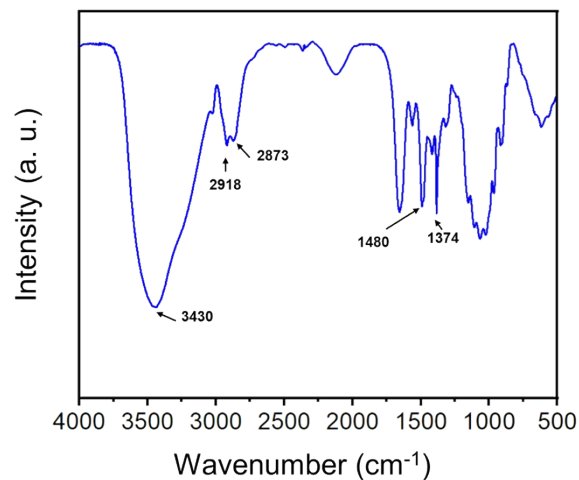
Figure S6. Figure S6. The FTIR spectra of QC. The FT-IR spectrum of QC showed the principal characteristic bands: the -OH stretching around 3430 cm^{-1}; while the weak absorption bands at wavenumbers 2918 cm^{-1} and 2873 cm^{-1} correspond to C-H stretching of hydrocarbon in the chitosan backbone. The peak around 1374 cm^{-1} corresponds to the C-O stretching of the amide group. The band at 1480 cm^{-1} corresponds to the methyl groups of ammoniums, confirming the quaternary ammonium salt modification. [2-4]
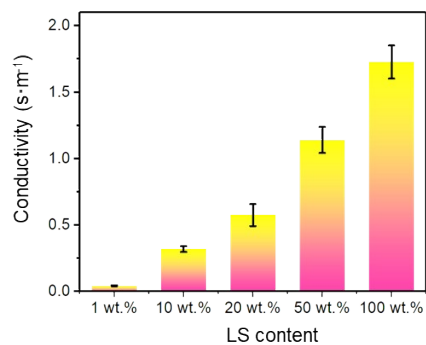
Figure S7. The conductivity of the LS solution. (Detailed composition can be seen in Table S3).

Figure S8. The compressive stress-strain curve of the various PVA-LS hydrogels.

Figure S9. Photographs and output voltage of devices with different size ($S=23.75$ cm^2).
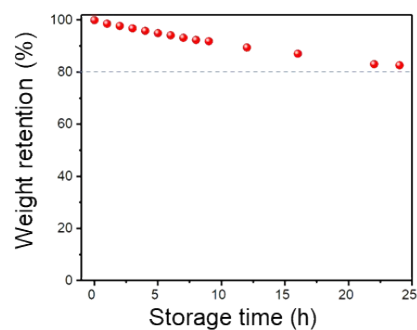
Figure S10. Weight retention of PVA-LS assembled PGHEG stored at 25 °C and 55 RH%.
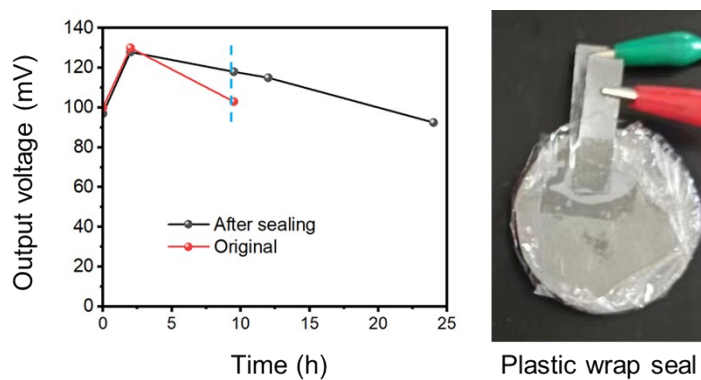
Figure S11. The plastic-sealed device demonstrates better output stability compared to the sample without protection.
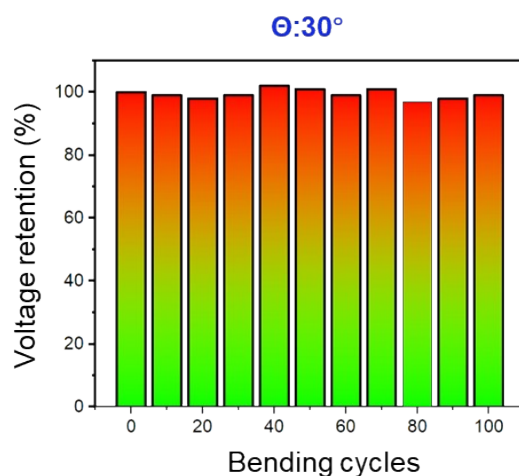
Figure S12. Voltage retention of PVA-LS assembled PGHEG after various bending

cycles at an angle of 30°.

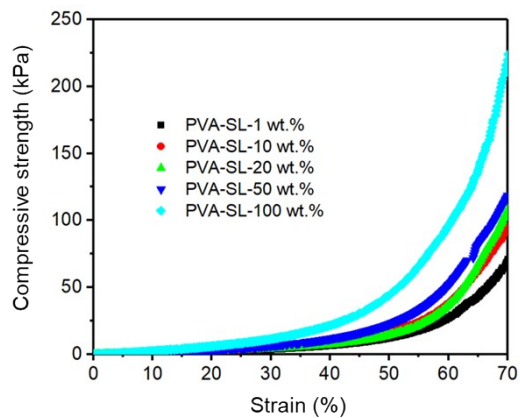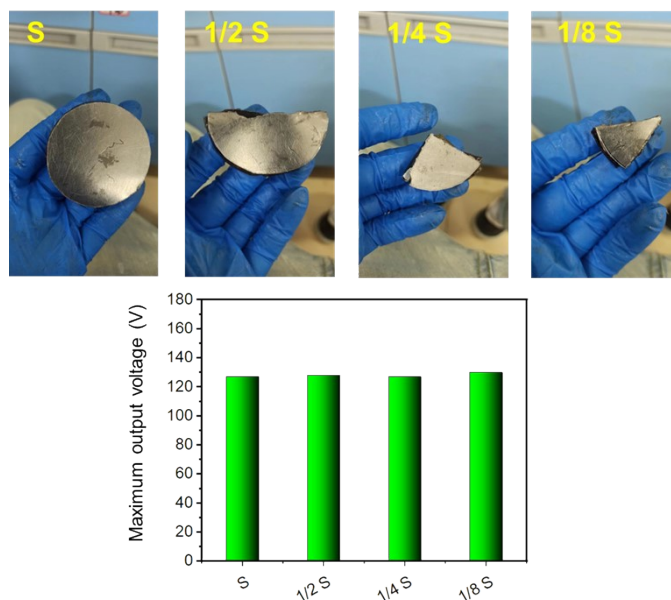During the cyclic bending of the device, the gel will be stretched and compressed, resulting in changes in the concentration of local ions. This will lead to small fluctuations in the voltage of the device. However, the output of the device is basically stable in the case of multiple cycles of bending, benefiting from the flexibility of the hydrogel.
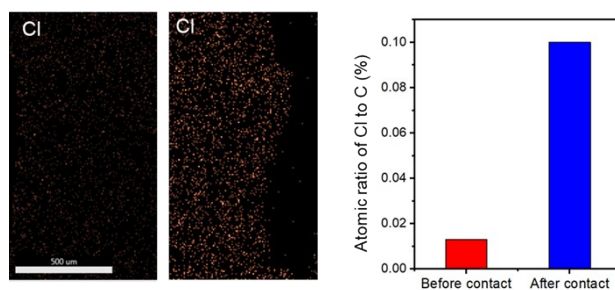
Figure S13. Changes in the Cl content of the original PVA hydrogel and the PVA

hydrogel that has been in contact with the PVA-QC hydrogel of PGHEG.
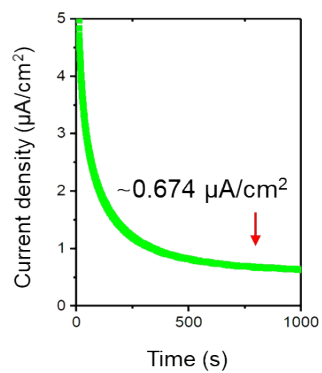
Figure S14. The real-time current of PGHEG assembled by PVA-QC (50 wt.%) hydrogel at room temperature.
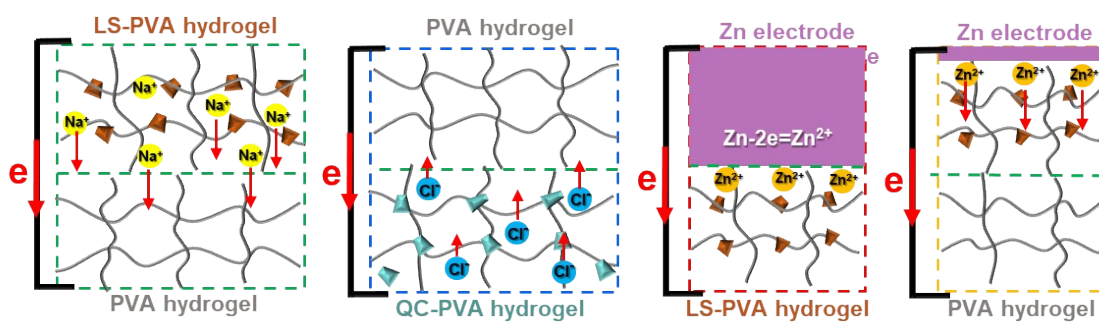
Figure S15. Schematic diagram of the electric-generation mechanism of the new integrated device.
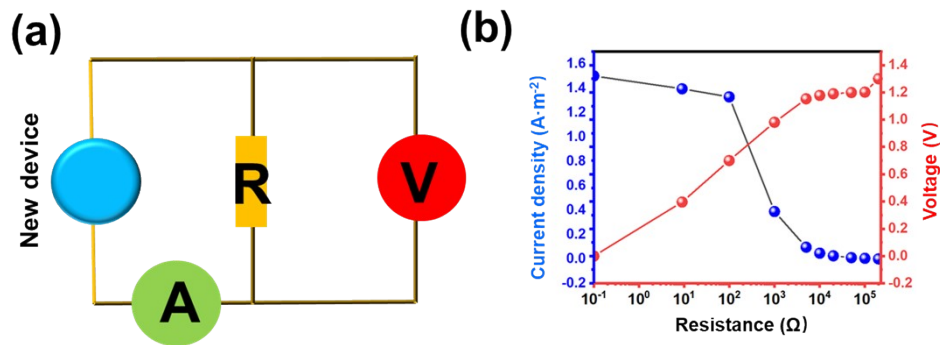
Figure S16. Electric output of the new device with the different electrical resistance as load. (a) Schematic diagram of the equivalent circuit for device power testing (b)Dependence of current density and voltage output on the electrical resistance of the external circuit.

The dependence of the voltage and current density on the electrical resistance of the external circuit is tested by connecting a device with a resistance box. The following equation calculates the power output:

P=UI

Where the "U" is the voltage tested on the resistance box. "I" is the current in the circuit calculated by Ohm's law.
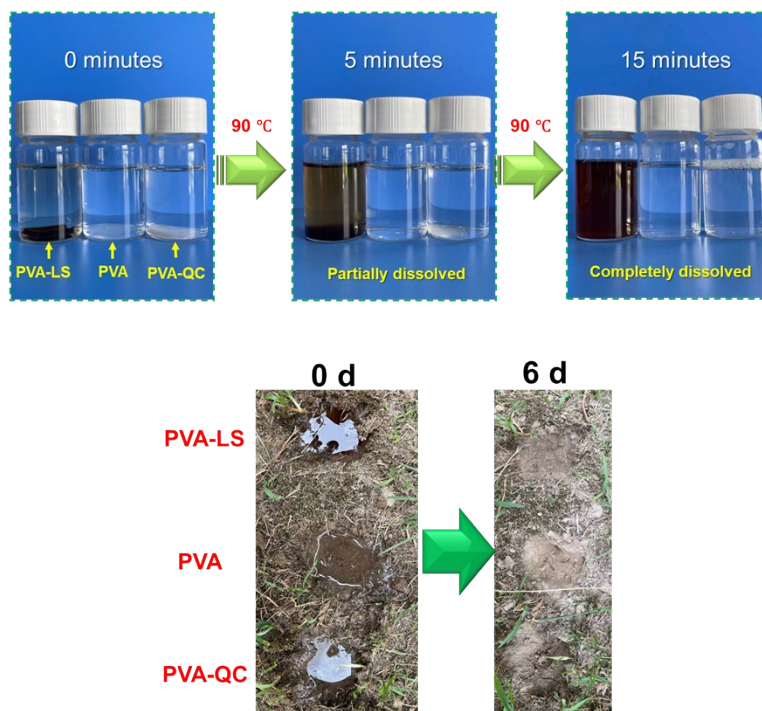
Figure S17. PVA-LS, PVA, and PVA-QC hydrogels ($1\times1\times0.5$ cm^3) can be quickly dissolved and recovered using hot water. The solution of the hydrogel components of the PGHEG device can be completely degraded in soil.

Experimental section

Preparation of PVA hydrogel

First, 1.5 g of polyvinyl alcohol powder (PVA-1799, Aladdin Industrial Corporation, Shanghai) was added to 8.5 g of deionized water and heated to dissolve completely. Then, the above solution was poured into a mold and frozen at -24 °C overnight, and then thawed for 4 h to obtain a PVA hydrogel. Normally, the hydrogel is stored in the refrigerator (4 °C). The detailed composition of the hydrogel can be seen in Table S1.

Preparation of PVA-LS hydrogel

First, 1.5 g of PVA-1799 and the appropriate amount of lignosulfonate sodium (LS, Aladdin Industrial Corporation) were added to 8.5 g of deionized water and heated to dissolve completely. Then, the above solution was poured into a mold and frozen at -24 °C overnight, and then thawed for 4 h to obtain a PVA-LS hydrogel. Normally, the hydrogel is stored in the refrigerator (4 °C). The detailed composition of the hydrogel can be seen in Table S1.

Preparation of PVA-QC hydrogel

First, 1.5 g of PVA-1799 and the appropriate amount of quaternary chitosan (QC, Kuer technology, Beijing) were added to 8.5 g of deionized water and heated to dissolve completely. Then, the above solution was poured into a mold and frozen at -24 °C overnight and then thawed for 4 to obtain a PVA-QC hydrogel. Normally, the hydrogel is stored in the refrigerator (4 °C). The detailed composition of the hydrogel can be seen in Table S33.

Characterization of LS and QC

1. The zeta potentials of the LS and QC were detected by a Malvern Zeta Sizer Nano ZS90 (UK) instrument. 2. The conductivity of LS and QC solution was measured using a PH meter (Thermo Fisher Scientific Co., Ltd.). 3. The morphology of the LS and QC was observed by scanning electron microscopy (SEM, Thermo Scientific Verios G4 UC).4. The FTIR spectra of LS and QC were measured with Nicolet 380 FTIR spectrometer (Thermo Electron Instruments Co., Ltd., USA).

Characterization of various hydrogels

The morphology of the PVA, PVA-LS (10 wt.%), and PVA-QC (10 wt.%) hydrogels was observed by scanning electron microscopy (SEM) with energy-dispersive X-ray analysis (EDAX) elemental mapping (AMETEK).

The PVA hydrogel is assembled with PVA-LS (10 wt.%) and PVA-QC (10 wt.%) hydrogels and connected to a commercial multimeter, respectively. Then the PVA hydrogel is freeze-dried and then subjected to elemental analysis.

Compression tests of the PVA-LS hydrogel

Cylindrical hydrogel samples are used for compression testing on a digital stretching machine (KJ-1065B, Kejian Instrument Co. Ltd, Dongguan, China). The compressive stress (CS) was calculated as

$$CS = F/A \ (1)$$

where F is the compressive load and A is the original area of the sample. The crosshead speed during compression was maintained at 10 mm/min.

The conductivity of the various hydrogel

The conductivity of various hydrogels was measured by an LCR meter (TH 2832), the applied voltage is 1 V, and the measurement frequency is 1 kHz. The conductivity (σ) is calculated by the following formula,

$$\sigma = L/RA \ (2)$$

in which R is the resistance, L and A are the materials' length and cross-sectional area, respectively[5].

Anti-dryness of the PGHEG

The PGHEG device is composed of PVA-LS (100 wt.%) hydrogel (S:23.74 cm^2, H:5 mm), PVA hydrogel (S:23.74cm^2, H:5 mm), and two graphite papers (electrode). This device is stored at 25 °C and 55 RH% to explore its anti-dryness ability.

Assembly of PGHEG devices

For anionic LS, PVA-LS hydrogels with various LS content (S: 23.74 cm^2, H: 5 mm) were placed on top of pure PVA hydrogels (S: 23.74 cm^2, H: 5 mm). Then, the double-layer hydrogel was sandwiched between two graphite paper (0.5 mm) electrodes to

assemble the PGHEG.

For cationic QC, PVA-QC hydrogels with different QC content (S: 23.74 cm^2, H: 5 mm) were placed under pure PVA hydrogels (S: 23.74 cm^2, H: 5 mm). Then, the double-layer hydrogel was sandwiched between two graphite paper electrodes (0.5 mm) to assemble the PGHEG.

We further placed the PVA-QC-100 wt.% hydrogel (S: 23.74 cm^2, H: 5 mm) under the PVA-LS-50 wt.% hydrogel (S: 23.74 cm^2, H: 5 mm) /PVA (S: 23.74 cm^2, H: 5 mm) hydrogel to make a sandwich structure. Then, the graphite electrode on the upper surface was replaced with an active Zn plate electrode. This is the integrated power generation device.

The electrical output performance of PGHEG

The open-circuit voltage (output voltage) of PGHEG is measured and collected using an electrochemical workstation (CHI 630E, Shanghai) and a commercial multimeter.

The short-circuit current (output current) of PGHEG is measured and collected using a source meter (Keithley Instrument Inc.). Note: the voltage must be set to 0 before the test.

The local ambient temperature is regulated by the refrigerator and oven.

Method S1

Thermodynamic analysis of mechanical-electrical conversion[5,6]

When the PVA-LS hydrogel touches the bottom PVA hydrogel, the double hydrogel will

form an LS gradient distribution. Due to the gradient distribution of LS or ionized Na^+, there are two migration modes of Na^+ in the bilayer hydrogel, namely (i) spontaneous diffusion of Na^+ from high concentration (hc) side to low concentration (lc) side and (ii) internal electric field-induced Na^+ from lc side to hc side. Among them, the diffusion current density can be expressed as follows.

$$J_{dif} = qFD\frac{dc}{dx} \quad (3)$$

where F is the Faraday constant, c, q, and D are the concentration of diffusion ions, valence, and diffusion coefficient of ions, respectively. Furthermore, the drifting current density can be defined as

$$J_{dri} = -qFcv\frac{dU}{dx} \quad (4)$$

$$v = D\frac{qF}{RT} \quad (5)$$

where v is the mobility of drifting ions, and U is the self-induced potential of gel. R is the gas constant, and T is the temperature.

The stable output potential (ΔU) of bilayer hydrogel can be obtained when the diffusion and drifting effects reach a dynamic balance (i.e., $J_{dri} = -J_{dif}$), which can be described as

$$\Delta U = \frac{RT}{qF}ln\frac{C(h)}{C(l)} \quad (6)$$

where $C(h)$ and $C(l)$ are concentrations of Na^+ at the hc side and lc side, respectively. This formula indicates that the intensity of the induced voltage (output voltage) is directly defined by the concentration gradient of Na^+, and the concentration gradient of Na^+ is

determined by the content of LS.

Supplementary Tables

Table S1. The compositions of PVA and PVA-LS hydrogels

	LS/PVA (wt.%)	PVA (g)	Deionized water (g)
PVA hydrogel	0	1.5	8.5
PVA-LS hydrogel	1	1.5	8.5
	10	1.5	8.5
	20	1.5	8.5
	50	1.5	8.5
	100	1.5	8.5

Table S2. The compositions of LS and QC solution

	QC (g)	LS (g)	Deionized water (g)
LS solution	0	0.015	8.5
	0	0.15	8.5
	0	0.3	8.5
	0	0.75	8.5
	0	1.5	8.5
QC solution	0.015	0	8.5
	0.15	0	8.5
	0.3	0	8.5
	0.75	0	8.5

Table S3. The compositions of PVA-QC hydrogels

	QC/PVA (wt.%)	PVA (g)	Deionized water (g)
PVA-QC hydrogel	1	1.5	8.5
	10	1.5	8.5
	20	1.5	8.5
	50	1.5	8.5

Table S4. Performance comparison between PGHEG and biological moist-generators/salt-gradient electric-generators

Material	Driving principle	Self-powered (if no, external input required)	Maximum voltage (mV)	Maximum areal current density ($\mu A\cdot cm^{-2}$)	Power density ($\mu W\cdot cm^{-2}$)	Ref.
Cellulose paper	Moist-electric	No, moisture	250	0.01	-	[7]
PVA-TA-CNTs hydrogel	Moist - electric	No, moisture	80	-	-	[8]
TEMPO-CNFs aerogel	Moist - electric	No, moisture	110	0.022	$0.63 *10^{-3}$	[9]
Silk cocoon membrane (Bombyx mori)	Moist - electric	No, moisture	31	0.0007	-	[10]
Silk membrane	Moist - electric	No, moisture	120	0.035	-	[11]
Asymmetric TEMPO-CNFs/ Quaternate NFs aerogel	Moist - electric	No, moisture	115	0.015	-	[12]
KCl-GG-agarose hydrogels	Salt-gradient-electric	Yes	177	-	-	[13]
AlCl$_3$- CNF-clay-PVA hydrogel	Moist - electric	No, moisture	78	-	-	[14]
PAM-AMPS-LiCl hydrogel	Moist - electric	No, moisture	0.81	480	53.3	[15]
PVA-PA hydrogel	Moist - electric	No, moisture	0.8	240	35	[16]
Zn/PVA-LS/PVA/PVA-QC hydrogel	**Polyelectrolyte-gradient-electric**	**Yes**	**1300**	**150**	**73.71**	**This work**

PVA: polyvinyl alcohol; **TA**: tannic acid; **CNTs**: carbon nanotubes; **TEMPO**:2,2,6,6-tetramethylpiperidine-1-oxyl;

CNFs: cellulose nanofibrils; **GG**: gellan gum; **PAM**: polyacrylamide; **AMPS**: 2-acrylamide-2-methyl propane

sulfonic acid; **PA**: phytic acid.

"—": not available in the references.

Reference

(1) Zhang, X.; Liu, W.; Yang, D.; Qiu, X. Biomimetic Supertough and Strong Biodegradable Polymeric Materials with Improved Thermal Properties and Excellent UV-Blocking Performance. *Advanced Functional Materials* **2019**, *29*, 1806912.

(2) Min, L.; Liu, M.; Liu, L.; Rao, Z.; Zhu, C.; Fan, L. Enzymatic synthesis of quaternary ammonium chitosan-silk fibroin peptide copolymer and its characterization. *International Journal of Biological Macromolecules* **2018**, *109*, 1125-1131.

(3) Wang, H.; Sun, Y.; He, T.; Huang, Y.; Cheng, H.; Li, C.; Xie, D.; Yang, P.; Zhang, Y.; Qu, L. Bilayer of polyelectrolyte films for spontaneous power generation in air up to an integrated 1,000 V output. *Nature Nanotechnology* **2021**, *16*, 811-819.

(4) Sajomsang, W.; Gonil, P.; Tantayanon, S. Antibacterial activity of quaternary ammonium chitosan containing mono or disaccharide moieties: Preparation and characterization. *International Journal of Biological Macromolecules* **2009**, *44*, 419-427.

(5) Lei, Z.; Wu, P. A highly transparent and ultra-stretchable conductor with stable conductivity during large deformation. *Nature Communications* **2019**, *10*, 3429.

(6) Zhao, F.; Cheng, H.; Zhang, Z.; Jiang, L.; Qu, L. Direct Power Generation from a Graphene Oxide Film under Moisture. *Advanced Materials* **2015**, *27*, 4351-4357.

(7) Gao, X.; Xu, T.; Shao, C.; Han, Y.; Lu, B.; Zhang, Z.; Qu, L. Electric power generation using paper materials. *Journal of Materials Chemistry A* **2019**, *7*, 20574-20578.

(8) He, P.; Wu, J.; Pan, X.; Chen, L.; Liu, K.; Gao, H.; Wu, H.; Cao, S.; Huang, L.; Ni, Y. Anti-freezing and moisturizing conductive hydrogels for strain sensing and moist-electric generation applications. *Journal of Materials Chemistry A* **2020**, *8*, 3109-3118.

(9) Li, M.; Zong, L.; Yang, W.; Li, X.; You, J.; Wu, X.; Li, Z.; Li, C. Biological Nanofibrous Generator for Electricity Harvest from Moist Air Flow. *Advanced Functional Materials* **2019**, *29*, 1901798.

(10) Tulachan, B.; Meena, S. K.; Rai, R. K.; Mallick, C.; Kusurkar, T. S.; Teotia, A. K.; Sethy, N. K.; Bhargava, K.; Bhattacharya, S.; Kumar, A.; Sharma, R. K.; Sinha, N.; Singh, S. K.; Das, M. Electricity from the Silk Cocoon Membrane. *Scientific Reports* **2014**, *4*, 5434.

(11) Yang, W.; Lv, L.; Li, X.; Han, X.; Li, M.; Li, C. Quaternized Silk Nanofibrils for Electricity Generation from Moisture and Ion Rectification. *ACS Nano* **2020**, *14*, 10600-10607.

(12) Yang, W.; Li, X.; Han, X.; Zhang, W.; Wang, Z.; Ma, X.; Li, M.; Li, C. Asymmetric ionic aerogel of biologic nanofibrils for harvesting electricity from moisture. *Nano Energy* **2020**, *71*, 104610.

(13) Lin, Z.-H.; Hsu, W.-S.; Preet, A.; Yeh, L.-H.; Chen, Y.-H.; Pao, Y.-P.; Lin, S.-F.; Lee, S.; Fan, J.-C.; Wang, L.; Chiu, Y.-P.; Yip, B.-S.; Lin, T.-E. Ingestible polysaccharide battery coupled with a self-charging nanogenerator for controllable disinfection system. *Nano Energy* **2021**, *79*, 105440.

(14) Hu, K.; He, P.; Zhao, Z.; Huang, L.; Liu, K.; Lin, S.; Zhang, M.; Wu, H.; Chen, L.; Ni,

Y. Nature-inspired self-powered cellulose nanofibrils hydrogels with high sensitivity and mechanical adaptability. *Carbohydrate Polymers* **2021**, *264*, 117995.

(15) Zhang, H.; He, N.; Wang, B.; Ding, B.; Jiang, B.; Tang, D.; Li, L. High-Performance, Highly Stretchable, Flexible Moist-Electric Generators via Molecular Engineering of Hydrogels. *Advanced Materials* **2023**, *35*, 2300398.

(16) Yang, S.; Tao, X.; Chen, W.; Mao, J.; Luo, H.; Lin, S.; Zhang, L.; Hao, J. Ionic Hydrogel for Efficient and Scalable Moisture-Electric Generation. *Advanced Materials* **2022**, *34*, 2200693.